

Energy Advances

Accepted Manuscript

This article can be cited before page numbers have been issued, to do this please use: C. K. Mytafides, W. J. Wright, R. Gustinvil, L. Tzounis, G. Karalis, A. S. Paipetis and E. Celik, *Energy Adv.*, 2024, DOI: 10.1039/D4YA00182F.



This is an Accepted Manuscript, which has been through the Royal Society of Chemistry peer review process and has been accepted for publication.

Accepted Manuscripts are published online shortly after acceptance, before technical editing, formatting and proof reading. Using this free service, authors can make their results available to the community, in citable form, before we publish the edited article. We will replace this Accepted Manuscript with the edited and formatted Advance Article as soon as it is available.

You can find more information about Accepted Manuscripts in the [Information for Authors](#).

Please note that technical editing may introduce minor changes to the text and/or graphics, which may alter content. The journal's standard [Terms & Conditions](#) and the [Ethical guidelines](#) still apply. In no event shall the Royal Society of Chemistry be held responsible for any errors or omissions in this Accepted Manuscript or any consequences arising from the use of any information it contains.

Additive manufacturing of highly conductive carbon nanotube architectures towards carbon-based flexible thermoelectric generators

View Article Online
DOI: 10.1039/D4YA00182F

Christos K. Mytafides^{1,2*}, William J. Wright¹, Raden Gustinvil¹, Lazaros Tzounis^{2,3}, George Karalis², Alkiviadis S. Paipetis², Emrah Celik^{1**}

¹ *Advanced Nano Systems Laboratory, Mechanical & Aerospace Engineering Department, University of Miami, 1251 Memorial Drive, FL 33146, Coral Gables, USA*

² *Composites and Smart Materials Laboratory, Materials Science & Engineering Department, University of Ioannina, GR-45110 Ioannina, Greece*

³ *Mechanical Engineering Department, Hellenic Mediterranean University, Estavromenos, 71004, Heraklion, Crete, Greece*

Abstract

Moving the fabrication of electronics from the conventional 2D orientation to 3D space, necessitates the use of sophisticated additive manufacturing processes which are capable to deliver multifunctional materials and devices with exceptional spatial resolution. In this study, it is reported the nozzle-guided 3D-printing of highly conductive, epoxy-dispersed, single-walled carbon nanotube (SWCNT) architectures with embedded thermoelectric (TE) properties, capable to exploit significant waste thermal energy from the environment. In order to achieve high-resolution and continuous printing with the SWCNT-based paste through a confined nozzle geometry, i.e. without agglomeration and nozzle clogging, a homogeneous epoxy resin-dispersed SWCNT paste was produced. As a result, various 3D-printed structures with high SWCNT concentration (10 wt %) were obtained via shear-mixing processes. The 3D printed *p*- and *n*-type epoxy-dispersed SWCNT-based thermoelements exhibit high power factors of 102 and 75 $\mu\text{W}/\text{mK}^2$, respectively. The manufactured 3D carbon-based thermoelectric generator (3D-CTEG) has the ability to stably operate at temperatures up to 180 °C in ambient conditions (1 atm, relative humidity: $50 \pm 5\%$ RH), obtaining TE values of an open-circuit voltage $V_{\text{OC}} = 13.6$ mV, short-circuit current $I_{\text{SC}} = 1204$ μA , internal resistance $R_{\text{TEG}} = 11.3$ Ohm, and a generated power output $P_{\text{MAX}} = 4.1$ μW at $\Delta T = 100$ K (with $T_{\text{Cold}} = 70^\circ\text{C}$). The approach and methodology described in this study aims to increase the flexibility of integration and additive manufacturing processes for advanced 3D-printed conceptual devices and the development of multifunctional materials.

* Corresponding author. Tel: [+30\(695\)500-5340](tel:+306955005340), [+1\(786\)819-1831](tel:+17868191831). E-mail: cmytafides@gmail.com (Christos K. Mytafides)

** Corresponding author. Tel: [+1\(305\)284-9364](tel:+13052849364). E-mail: e.celik@miami.edu (Emrah Celik)



Keywords: Carbon-based Thermoelectric Generator (CTEG); Additive Manufacturing; 3D-Printed Thermoelectric Generator (3D-TEG); Single-Walled Carbon Nanotubes (SWCNTs); Energy-harvesting devices;

View Article Online
DOI: 10.1039/D4YA00182F

Highlights:

- SWCNT/epoxy-based p-type 3D-printed TE material with power factor $102 \mu\text{W}/\text{mK}^2$
- SWCNT/epoxy-based n-type 3D-printed TE material with power factor $75 \mu\text{W}/\text{mK}^2$
- Open circuit voltage of 3D-CTEG: $V_{\text{OC}} = 13.6 \text{ mV}$
- Short circuit current of 3D-CTEG: $I_{\text{SC}} = 1204 \mu\text{A}$
- Power output of 3D-CTEG: $P_{\text{max}} = 4.1 \mu\text{W}$

1. Introduction

Among the most urgent concerns we encounter daily are those related to the environment and energy consumption. Vast amount of energy is lost in terms of heat when it is converted from the primary carriers to the end use. Waste energy generated as heat worldwide by the most prevalent end use sectors including residential, industrial, transportation, and power plants globally, account for nearly 72 percent of worldwide energy supply. More specifically, 63 percent of the aforementioned heat energy is generated at temperatures below $100 \text{ }^\circ\text{C}$. The power generation field has the highest proportion in this temperature range, followed by industries and transportation [1]. Better utilization of this excessive thermal energy has the potential to improve the energy efficiency minimizing the consumption. Thermoelectric (TE) generation is a quite promising renewable energy technology with a broad variety of potential applications. Thermal energy conversion to electricity is a sustainable energy source that may be utilized to exploit waste dissipated heat by leveraging the Seebeck effect of thermoelectricity [2]. TE materials with high Seebeck coefficient (S) demonstrate high thermoelectric energy generation since the thermoelectric voltage (V) is related to the temperature variation (ΔT) according to the equation of $S = \Delta V / \Delta T$. In addition, the power factor (PF) is defined as $PF = \sigma \cdot S^2$, where σ is the electrical conductivity and S is the Seebeck coefficient, and is used to measure the efficiency of a TE material.

In addition to high Seebeck coefficient and high electrical conductivity, TE material must have low thermal conductivity to effectively transform waste heat into useful power. A low thermal conductivity is needed to maintain a substantial temperature difference within the material [3, 4]. Even though TE materials have the potential to provide an efficient and reliable renewable technology theoretically, the majority of materials that currently render the highest efficiency are costly to produce and are based on components that are rare in nature or/and toxic. Tellurium, bismuth, lead



telluride, bismuth telluride, zinc antimonide, silicon, and germanium are some of the most commonly used TE materials [5, 6]. Typical thermoelectric materials and module production is a tedious multi-step procedure which comprises material production and synthesis, casting of thermoelements and metal interconnection of these thermoelements which mandates the employment of advanced instrumentation. In addition, this processing method has various limitations, including the fact that it is only adaptable to rectangular designs where a considerable proportion of the active material is lost during the manufacturing process. In addition, large scale integration requires significant amount of time [7, 8]. As a result, the cost of thermoelectric energy generation escalates significantly. This is indicative of the fact that there is a lack for commercial demand for thermoelectric generators (TEGs). TEGs have a great potential use in remote energy-harvesting and the supply of power for wireless and portable devices, and they might make a substantial contribution to the field of Internet of Things (IoT). To accomplish these goals, the weight, the design as well as the form-factor of the TE devices (i.e. flexibility) become crucially important in addition to the cost and the device performance. This dictates the necessity for simple processes based on low-cost carbon-based TE materials that may be printed in order to manufacture flexible and organic or carbon-based TE devices [9, 10]. Currently, TE materials are of great attention from the scientific community and numerous of organic and inorganic materials are being investigated as potential materials for thermoelectric energy-harvesting devices [11-14].

Additive manufacturing (or 3D printing) technology provide substantial assets in terms of reducing the cost, equipment, time and difficulty of thermoelectric material and device production. Furthermore, it is capable to produce sophisticated and adaptable device geometries as well as flexible and adjustable manufacturing parameters [6]. TE materials may be printed in a layer-by-layer fashion via a computer-aided procedure, simplifying the manufacturing process, minimizing the product-waste as well as maximizing the freedom of the shape-printing and device design. Additive manufacturing methods have recently been employed to produce TE materials in the form of thick components or thin films.

Inkjet printing and screen printing, for example, have been shown to be effective methods for effortlessly changing geometrical parameters like size and shape [6, 15-19]. However, because of their high porosity, these approaches demonstrate limited power output, high contact resistance between the thermoelements, and poor mechanical characteristics. These limitations can be alleviated by printing thicker and denser components.

TEGs made from bismuth-telluride were created utilizing the screen-printing technology and extrusion-based printing [20, 21]. Accordingly, He et al. showed the manufacturing of TE bismuth-antimony-telluride nanoparticle-based (NPs) samples in photo-resin using stereolithography in ratios



containing up to 60% NPs. The 3D-printed thermoelements can mostly consist of NPs after thermal annealing [22]. Stereolithography and dispenser-printing methods are auspicious additive manufacturing processes for the production of thick TE components. Nonetheless, both exhibit inadequate TE efficiency comparing to standard manufacturing processes, with orders of magnitude lower TE characteristics.

Furthermore, selective laser melting (SLM) and sintering (SLS) are two developing technologies that have recently been used to produce thermoelements with complicated shapes and designs [23, 24]. These methods rely on the deposition of a thin layer of thermoelectric powder, followed by melting with a laser beam and solidification [25, 26]. Notwithstanding the ability to fabricate thermoelectric materials with various shapes, such procedures need a significant initial investment in equipment [27] limiting the adoptability of these manufacturing processes.

Carbon-based printable materials are of great interest as they are inexpensive to produce, they are abundant, non-toxic, and their low density is beneficial for high specific energy output. Single-walled carbon nanotubes (SWCNTs) [28] possess unique electrical, mechanical, and thermal characteristics and they can be prepared inexpensively in the form of conductive or semiconductive inks for the fabrication of printed electronics [29]. SWCNTs are commonly used as additives to increase the conductivity of polymers, which are usually employed for 3D-printing materials. One of the most challenging issues in the field of 3D-printed electronics is determining the optimal printing procedure for manufacturing high resolution 3D structures. Recent studies have demonstrated the fabrication of 3D elements in the scale of micrometer utilizing the ink-based printing techniques. In addition, SWCNTs have attracted particular interest as raw materials for the development of printed electronics and thermoelectric generators [30-32]. This is due to both their significant phonon scattering capabilities and their exceptionally high electrical and mechanical properties. Furthermore, SWCNTs have adjustable semiconducting qualities since their *n*- or *p*-type behavior may be altered using certain doping techniques, resulting in noteworthy adaptability in terms of TE properties [33, 34].

In this study, it is demonstrated the manufacturing process and the performance of a flexible carbon-based 3D-printed thermoelectric generator (3D-CTEG) approaching a low-cost and versatile production of energy harvesting devices. Single-wall carbon nanotubes (SWCNTs) were used for the production of the printable pastes which were mixed with a flexible epoxy resin to realize self-standing thermoelectric elements, in order to fabricate the 3D-CTEG with significant TE performance. The successful implementation of the carbon-based additively manufactured flexible TE systems, reduces current costs and geometric limitations and allows for a wide range of applications of these materials.

2. Materials and Methods

2.1. Preparation of SWCNT-based TE paste

Single-walled carbon nanotubes powder (purity of carbon $\geq 85\%$) was acquired from OCSiA (TUBALL™, Russia) with approximately $5\mu\text{m}$ length and 1.7 ± 0.5 nm outer mean diameter. The p-type TE ink was produced by a facile epoxy-based solution/mixing process, by adding SWCNTs and poly(3,4-ethylenedioxythiophene) polystyrene sulfonate (PEDOT:PSS) in the Superflex (flexible-after-curing) epoxy resin (3DMaterials, Korea) as presented in Figure 1a-c. The mixture of 10 wt% of SWCNTs and 5 wt% of PEDOT:PSS in the epoxy was mixed utilizing the ARM-310 shear mixer (Thinky Corporation, Japan) primarily for 5 minutes, then for another 7 minutes. All mixing processes using the ARM-310 were performed at 2000 rpm, resulting in viscous SWCNT-based thermoelectric inks/pastes of 27 Pa·s. The n-type SWCNT-based 3D-printed thermoelement was produced by adding 10 wt% SWCNTs and 10 wt% polyethylenimine (PEI) in the Superflex epoxy resin. In this work, PEI was used as a low-cost, air-stable, and easy to process *n*-dopant. PEDOT:PSS and PEI were acquired from Sigma-Aldrich (Merck, Germany). After the SWCNT/epoxy-based TE pastes were produced, it were successfully extruded utilizing the direct ink writing (DIW) method as can be seen in Figure 1a-c, using a 0.8 mm nozzle at 345 kPa. The printing process of the 3D-CTEG thermoelements, were performed at 30 mm/s on forward/backward order, creating 3 uniform layers. Each printed line of the SWCNT-based material was in contact with air for 0.9 to 4.5 ± 0.2 seconds before forming into an entire thermoelement. The SWCNT/epoxy-based thermoelements were cured in an oven at $100\text{ }^\circ\text{C}$ for 2 hours, demonstrating a remarkable flexibility for an epoxy-based solid and cured material as shown in Figure 1e-f. For high-grade 3D-printable materials with significant TE efficiency, it is essential to produce dispersions with qualitative characteristics such as the viscosity which significantly contributes to the self-standing printing during the additive manufacturing process [35, 36]. Figure 1 shows the production process and the 3D-printed SWCNT-based materials, as well as the additive manufacturing process towards the 3D-printed flexible thermoelements.



Figure 1. Thermoelectric paste production process. (a) The dispersion process of the SWCNTs using a shear-mixer, (b) the produced p-type SWCNT/epoxy-based dispersion after extrusion printing, (c) the additive manufacturing process of thermoelements, (d) the thermoelectric characterization of the 3D-printed materials and (e-f) the flexibility of the SWCNT/epoxy-based 3D-printed TE material after curing.

2.2. Fabrication of the 3D-CTEG module

A flexible carbon-based 3D-printed TEG device was manufactured via facile paste printing processes utilizing the produced materials, consisted of 2 *p*-/*n*-pairs. Figure 2a, illustrates the additive manufacturing of TE module fabrication process. The 3D-CTEG *p*-/*n*-pair has the dimensions of 13 mm × 15 mm × 2.0 mm as indicated in Figure 2b. Initially, *p*-type TE material was 3D-printed on a scaled PTFE/Teflon substrate in order to print-develop the device design architecture. Thereafter, *n*-type material printing was processed in the same way on the same substrate to alternate the carbon-based interconnection resulting in a continuous electric path composed of 2 *p*-/*n*- pairings. Copper foils were integrated directly while printing the *p*- and *n*-type carbon-based materials on top of the copper as the anode and cathode terminals of the device. All the thermoelements were cured at 100 °C for 120 minutes after printing. The 3D-printed highly-dense and conductive SWCNT network was also employed as electrodes/interconnections between the printed thermoelements, resulting in a carbon-based TEG that does not require metal deposition as it is also described in a previous study [13], where the contact resistance between the metal electrode and the SWCNTs is larger in the case of highly electrically conductive SWCNTs than the resistance of the metal or the SWCNT itself, and as a result, the procedure adding metallic interconnections in large scale results in TEGs with lower power output [37]. The carbon-based 3D-printed TEG and its working principle are illustrated in Figure 2c-d.



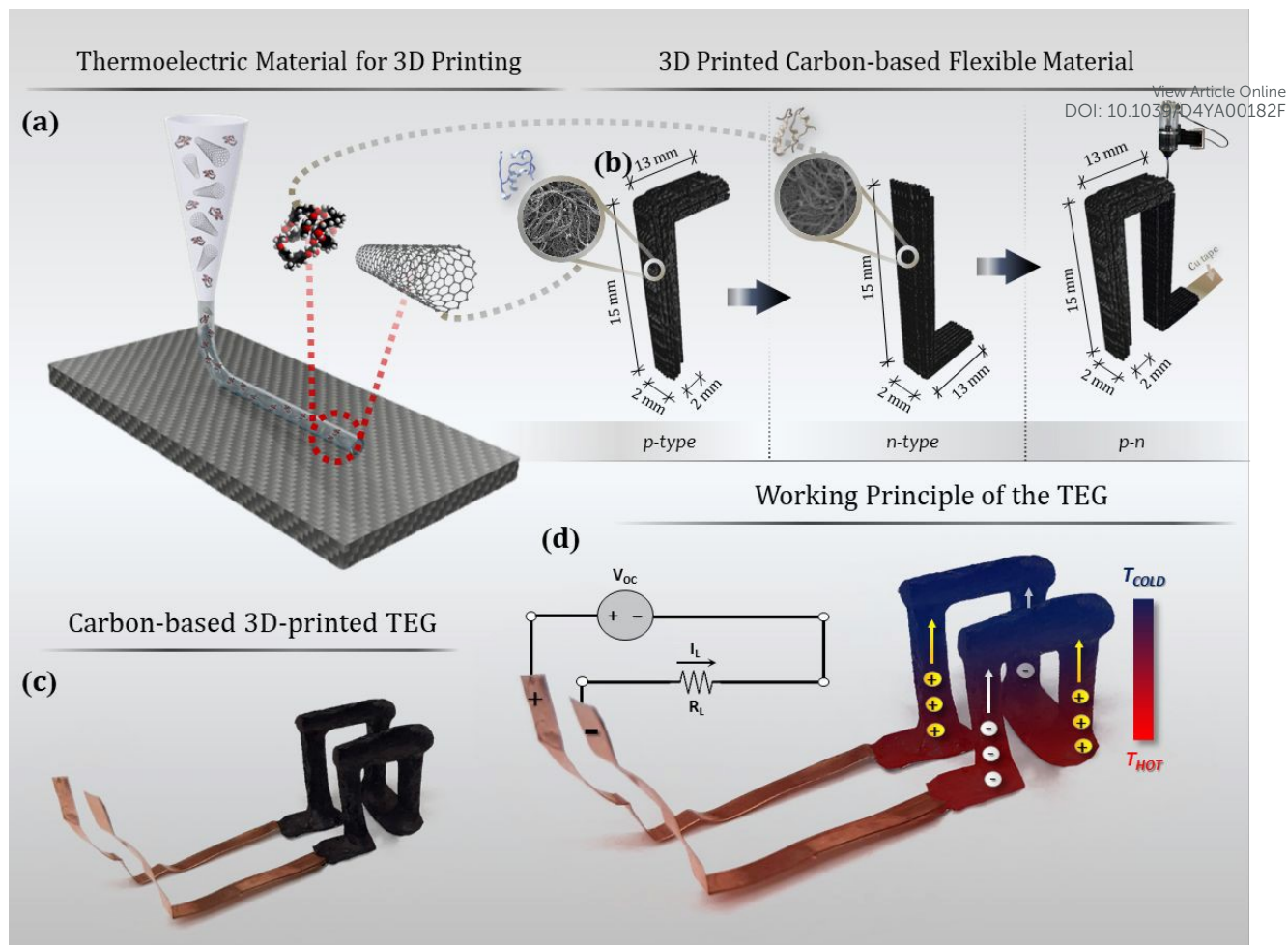


Figure 2. Carbon-based 3D-printed flexible TEG manufacturing process. (a) Additive manufacturing process of the SWCNT/epoxy-based TE materials, (b) printing process and dimensions of the thermoelements of the CTEG device, (c) 3D-CTEG device architecture, (d) schematic illustration of the thermoelectrically generated carriers, by a given temperature difference (ΔT) as well as the 3D-CTEG's module working principle and the CTEG's equivalent circuit.

2.3. Characterization, thermoelectric properties and performance measurements

Surface morphological micrographs of the 3D-printed TE materials were taken using a Zeiss Gemini Field Emission Scanning Electron Microscope (FE-SEM), operating at an accelerating voltage of 1.0 to 3.0 kV (Zeiss, Germany). In order to characterize the thermoelectric properties of the fabricated 3D-CTEG module, the performance and the thermal stability of the materials were carried out. The thermopower was generated by keeping one block “cold” at room temperature (i.e. $T_{\text{ambient}} \sim 25^\circ\text{C}$) while heating the other at various temperatures. The measurements were performed in a laboratory environment at 1 atm pressure and relative humidity of $50 \pm 5\%$. The temperatures of T_{Cold} and T_{Hot} blocks were continuously controlled by K-type thermocouples and a Digital IR Thermometer OS-VIR50 (OMEGA Engineering Ltd., United Kingdom) for the accurate temperature difference (ΔT) monitoring. 3D-CTEG's current and voltage generated under various temperature differences, were measured using the 34401Agilent DMM (Agilent Technologies, USA). Viscosity measurements of the thermoelectric materials have been performed using the NDJ-9S digital viscometer. The efficiency



and the performance of the flexible 3D-CTEG was computer-controlled by custom made LabVIEW programs in order to deliver the V-I, P-I, V-Load and P-Load curves.

View Article Online
DOI: 10.1039/D4YA00182F

The electrical conductivities, Seebeck coefficients, power factors and figure of merits (ZTs) of the 3D-printed SWCNT-based thermoelements were measured using the Linseis LSR-3 thermoelectric characterization instrument (Linseis, Germany). The reported values are average values from at least five measurements carried out on different samples. The thermal conductivities of the produced materials were determined utilizing the Linseis THB-100 instrument under various temperature differences (Linseis, Germany). The thermal behavior of the produced materials was examined by using the STA 409 CD thermogravimetric analyser from NETZSCH GmbH (Selb, Germany), where the specimens were placed in a ceramic crucible and heated up with a constant heating rate of 10 °C/min in an oxygen atmosphere under a constant gas flow of 60 ml/min.

3. Results and Discussion

3.1. *Thermoelectric properties and characterization of the developed materials*

For the purpose of fabricating optimized p- and n-type 3D-printed thermoelectric structures, various SWCNT:additive mass ratios were investigated, initially utilizing flexible epoxy as a dispersion medium to create conductive 3D-printable inks, and then modified and investigated accordingly with various additive:mass-ratios to achieve preferable viscosity and thermoelectric characteristic to manufacture 3D flexible TEG architectures. In particular, Figure 3a, illustrates the achieved viscosities of the developed thermoelectric TE materials at various epoxy:SWCNTs mass ratios at room temperature. The initial epoxy:SWCNTs developed material achieved the viscosity of 27 Pa·s. Figure 3b-c depicts the recorded Seebeck coefficients, power factors and electrical conductivities of the produced p- and n-type SWCNT TE materials at various mass ratios, measured as cured structures. While developing the SWCNT dispersions, the optimum ratio regarding the TE properties and the viscosity for the 3D-printing process were the 10 wt% of SWCNTs / 20 wt% of PEDOT:PSS in the epoxy for the p-type, and 10 wt% of SWCNTs / 15 wt% of PEI for the n-type material. As referred [32, 38, 39] and also observed in the this study, the use of PEDOT:PSS prevents nanotube-epoxy interactions and any unwanted n-doping modification due to the amine-groups containing in epoxy resins. For the n-type fabrication while using PEI, it has been investigated that when the mass ratio of PEI to SWCNTs exceeds 10:15, the Seebeck coefficient does not provide any significant enhancement while the electrical conductivity decreases significantly as more dielectric PEI molecules interact with the conductive nanotubes. Apart from being high-quality and homogeneous dispersions, the selected TE pastes, also exhibiting the quite satisfactory functional viscosities for 3D printing of 25 Pa·s and 29 Pa·s, for p- and n-type respectively, as shown in Figure 3a. As a result, they may also be employed for large-scale printing processes.



In this study, environmentally friendly methods were acquired to produce TE pastes for facile 3D-printed applications, avoiding the use of heavy chemicals and strong acids for dopants as has been previously referred in other studies [40, 41]. Figure 3 depicts the electrical conductivities of 579 S/cm and 434 S/cm and the Seebeck coefficients of 36 $\mu\text{V/K}$ and $-35 \mu\text{V/K}$ were obtained of p- and n-type structures. As a result, the recorded PFs were as high as 75 $\mu\text{W/mK}^2$ and 54 $\mu\text{W/mK}^2$ at $\Delta T=100\text{K}$ for the developed p- and n-type SWCNT-based flexible 3D-printed materials, respectively.

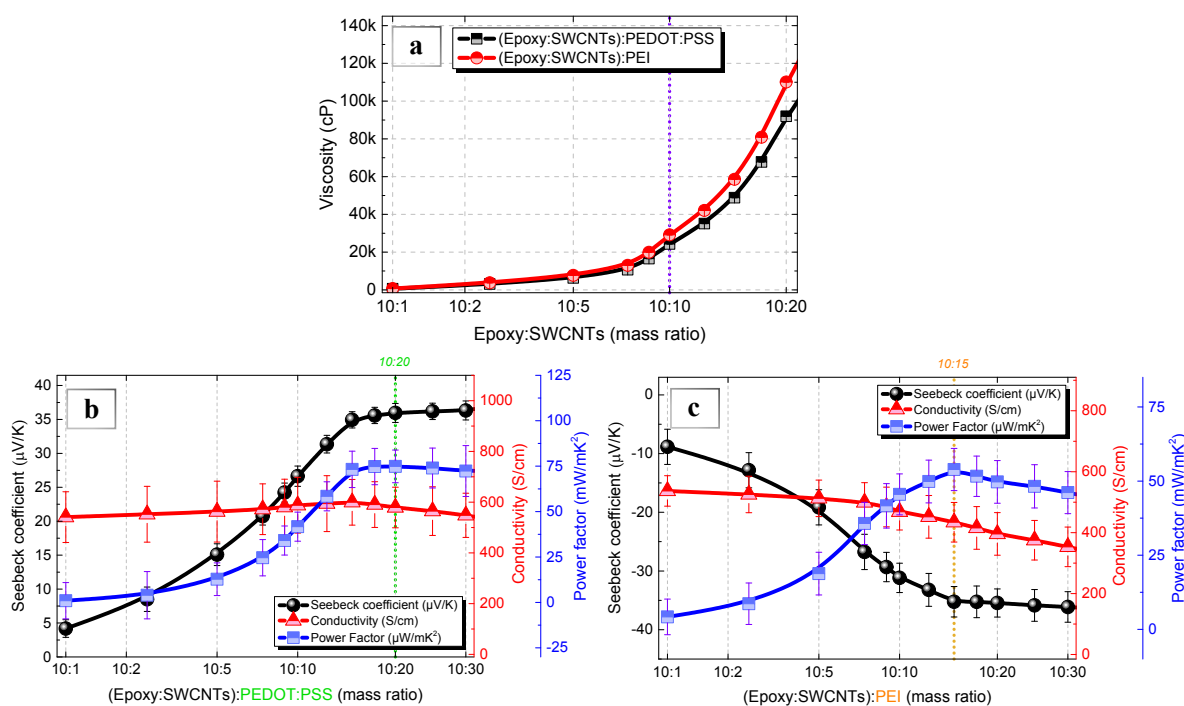


Figure 3. Thermoelectric characterization of the 3D-printed TE materials. (a) Viscosities of the produced additive manufacturing SWCNT/epoxy-based TE materials at various mass ratios at room temperature, and (b,c) Seebeck coefficients, electrical conductivities, and power factors of the p- and n-type printed structures at various (Epoxy:SWCNTs):Additive mass ratios.

3.2. Thermogravimetric analysis of p- and n-type materials

Thermogravimetric analysis (TGA) was performed to evaluate their thermal performance and limitations of the 3D-printed p- and n-type SWCNT/epoxy-based TE materials. This thermal investigation demonstrates the capacity and stability of the produced 3D materials for low temperature applications up to 180 $^{\circ}\text{C}$. Figure 4a shows the thermal degradation of the materials in terms of their weight mass. Zone “I”, represents the evaporation of water in each material (0-210 $^{\circ}\text{C}$), whereas zone “II” indicates the initiation of polymer molecules burning (210-500 $^{\circ}\text{C}$), and zone “III” illustrates the beginning of SWCNT degradation and also the combustion of the residual polymer molecules (500-1000 $^{\circ}\text{C}$). This is also consistent with the initial SWCNTs as shown in Figure 4a-b.



To summarize, the PEI-based n-type 3D-printed SWCNT/epoxy-based material, demonstrates a stable but highly depended to high-temperature limit at 180°C, making it ideal for low-temperature applications, such as biothermal or wearable energy harvesting devices. The remaining ~15% of mass on SWCNT-based TGA samples is related to metal impurities produced during the nanotube fabrication process [42].

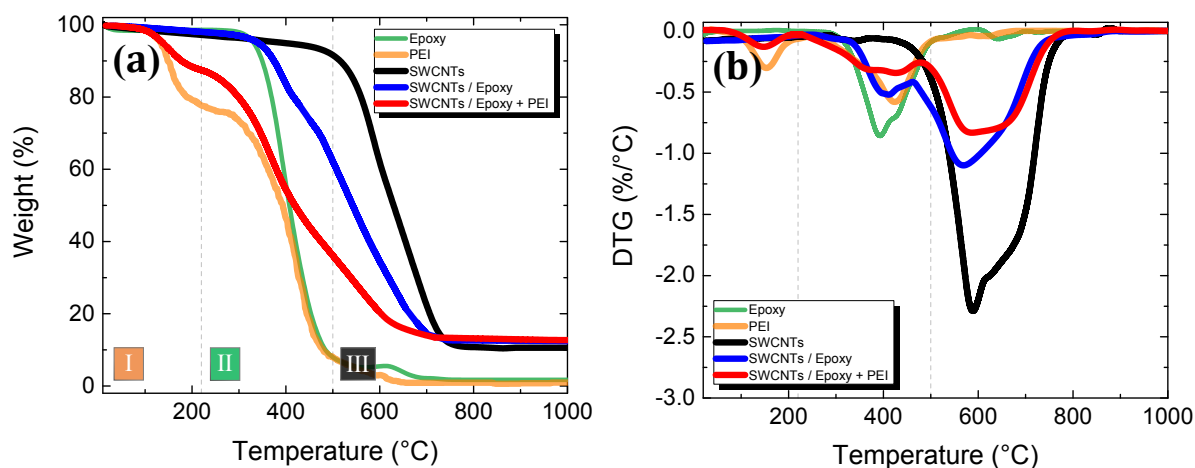


Figure 4. (a) Thermogravimetric analysis (TGA) and (b) the derivative of TG (DTG) of p-type, n-type thermoelements, Epoxy, PEI and pristine SWCNTs.

3.3. Surface morphology and microscopy characterization of the 3D-printed materials

The solid-state morphology and the dispersion quality of the 3D-printed SWCNT/epoxy-based n- and p-type TE materials were investigated. Figure 5 depicts the SEM images of the surface morphology of the n- and the p-type 3D-printed structures. As mentioned before, the SWCNT/epoxy mixtures were produced utilizing a shear-mixer at 2000rpm, 3D-printed via DIW and cured at 100°C for 2 hours. The three-dimensional printed structures demonstrate comparable dense-network structures that efficiently assist to carrier transports, implying to the functionalized thermoelectric dispersions of the produced n- and p-type materials. Figure 5a-b illustrates the remarkable continuity of the SWCNT network of the p-type printed material. Figure 5c-d shows the n-type printed structure, where an excellent doping of SWCNTs was established during the thermoelectric characterization as described in paragraph 3.4, confirming that adequate PEI molecules were bonded on the surfaces of the SWCNTs, leading in efficient doping due to the anion-induced electron transfer between the nitrogen anions (N^-) of PEI to the SWCNTs. In an earlier study, it is also mentioned the effective n-doping of utilizing PEI molecules on SWCNTs [37, 43, 44].



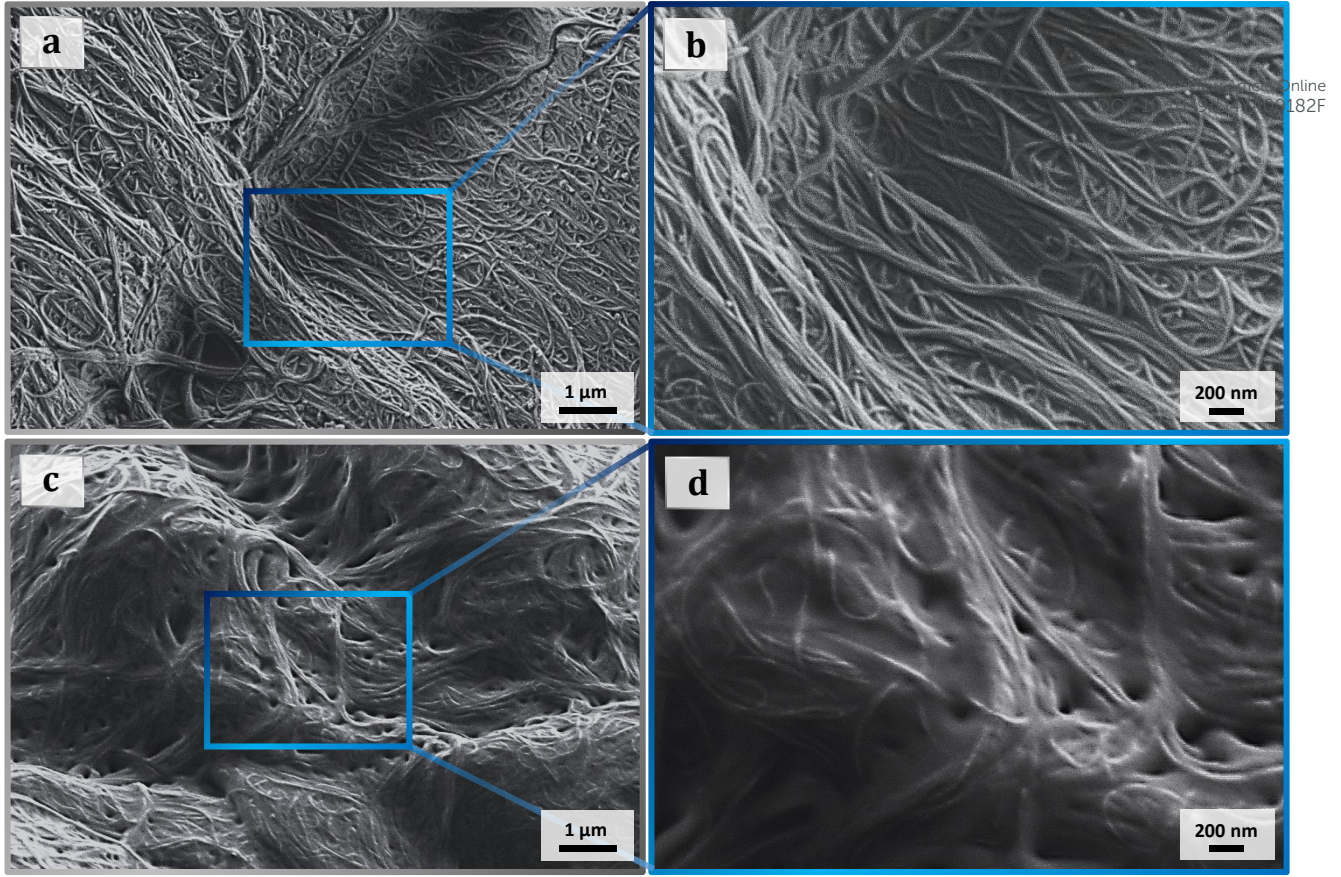


Figure 5. (a,b) SEM micrographs of the p- and (c,d) n-type 3D-printed SWCNT/epoxy-based TE materials.

3.4. Thermoelectric characterization of the carbon nanotube-based 3D printed materials

The thermoelectric characteristics of the SWCNT/epoxy-based 3D-printed materials were thoroughly investigated. More specifically, the σ : electrical conductivity, S : Seebeck coefficient, PF : power factor, κ : thermal conductivity, zT : figure of merit, and η : thermoelectric efficiency of the 3D-printed materials were measured or evaluated as a function of temperature. The dimensionless figure of merit (zT) of a TE material that is used to describe the TE efficiency is equal to [11]:

$$zT = \frac{\sigma S^2 T}{\kappa} \quad (1)$$

where σ , S , κ , are as described above, and T is the absolute temperature. For a TE material, the ideal efficiency of thermal to electrical energy conversion is stated as [45]:

$$\eta = \left(\frac{T_H - T_C}{T_H} \right) \frac{\sqrt{1 + Z\bar{T}} - 1}{\sqrt{1 + Z\bar{T}} + (T_C/T_H)} \quad (2)$$

The Carnot efficiency is described by the first factor in (2). The second factor specifies how much Carnot efficiency may be produced from a TEG under a certain ΔT , which is a function of $Z\bar{T}$. T_H



denotes the temperature at the hot surface, whereas T_C denotes the continuous temperature of a cool surface. The temperature differential ($T_H - T_C$) of a TE material is defined by the temperatures on its hot side (T_H) and cold side (T_C), and \bar{T} is the average of these values.

Figure 6a,b depicts the TE performance of the p-/ and n-type SWCNT/epoxy-based materials as a function of T . The remarkable values of 620 S/cm and 471 S/cm, as well as the significantly high S values of 41 $\mu\text{V/K}$ and $-40 \mu\text{V/K}$ at $T=180^\circ\text{C}$ are notable. As a consequence, the 3D-printed p- and n-type SWCNT/epoxy-based TE materials have the substantial PF s of $102 \mu\text{W/mK}^2$ and $75 \mu\text{W/mK}^2$, respectively. The obtained κ values for the 3D-printed TE structures are 0.174 W/mK and 0.132 W/mK for the p- and n-type materials, respectively, and decline as the temperature rises, which is consistent with earlier findings, reaching the values of 0.09 W/mK and 0.07 W/mK respectively at $T=180^\circ\text{C}$ [13, 46, 47]. Ultimately, the significant zT of 0.52 and 0.47 at $T=180^\circ\text{C}$ give remarkable conversion efficiencies of $\eta=3.4\%$ and $\eta=2.9\%$ for the p- and n-type TE materials respectively. These values herald a quite promising future of additive manufacturing in thermoelectrics, as they arise from abundant, low-cost, flexible carbon-based and facile to manufacture materials.

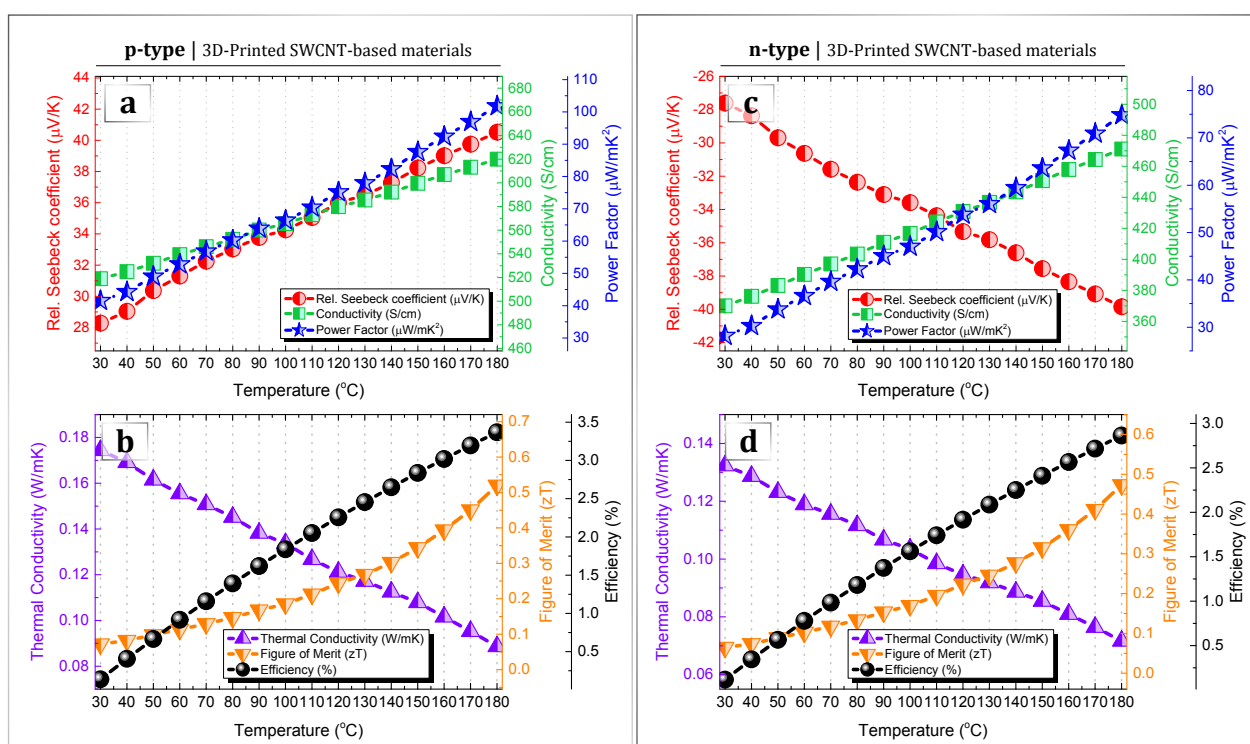


Figure 6. Thermoelectric characterization and properties of the 3D-printed SWCNT-based materials. (a,c) The measured Seebeck coefficients, electrical conductivities, power factors, and (b,d) thermal conductivities, zT and thermoelectric efficiencies of (a,b) p- and (c,d) n-type epoxy-dispersed nanotube-based TE materials respectively at various temperatures.

3.5. Performance and demonstration of the 3D-CTEG device



The fabricated 3D-CTEG device exhibited a significant thermoelectric performance, due to the excellent characteristics of the n- and p-type 3D-printed materials, manufactured employing the SWCNT/epoxy-based semiconducting materials via DIW method. When the 3D-CTEG module is exposed to a ΔT between the device's top and bottom sides (through-thickness), a significant power output is generated. The experimentally measured TE performance of the 3D-CTEG device in multiple ΔT s is illustrated in Figure 7. The measurements were conducted under standard laboratory conditions ($T:25^{\circ}\text{C}$, $\text{RH}: \sim 50\%$, 1atm). The printed architecture of the flexible 3D-CTEG having the dimensions of $13\text{ mm} \times 13\text{ mm} \times 15\text{ mm}$, demonstrated a total thermopower of $136\ \mu\text{V/K}$ at $\Delta T=100\text{K}$. It should be noted that the fabricated 3D-CTEG displayed an excellent TE performance for each thermoelement without the need of metallic interconnections. This result was achieved due to the superior conductivity of the SWCNT-based 3D-printed materials, as well as the short distance between the linked thermoelements. As has been referred in a previous study, the contact resistance of a metallic interconnection and a printed nanotube-based structure is larger than the internal resistance of either a metal or a SWCNT-based structure alone, resulting in a reduced power output [13, 37]. This is not the case with our 3D-CTEG, which is made entirely of SWCNTs with high electrical conductivity. At $\Delta T=100\text{ K}$, a $V_{\text{OC}}=13.6\text{ mV}$ (open-circuit voltage) and an $I_{\text{SC}}=740\ \mu\text{A}$ (short-circuit current) were obtained during the 3D-CTEG performance measurements with an internal resistance $R_{\text{TEG}}=11.3\ \text{Ohm}$. This resulted in a significant power output of $4.1\ \mu\text{W}$, as can be seen in Figure 7 and Figure 8.

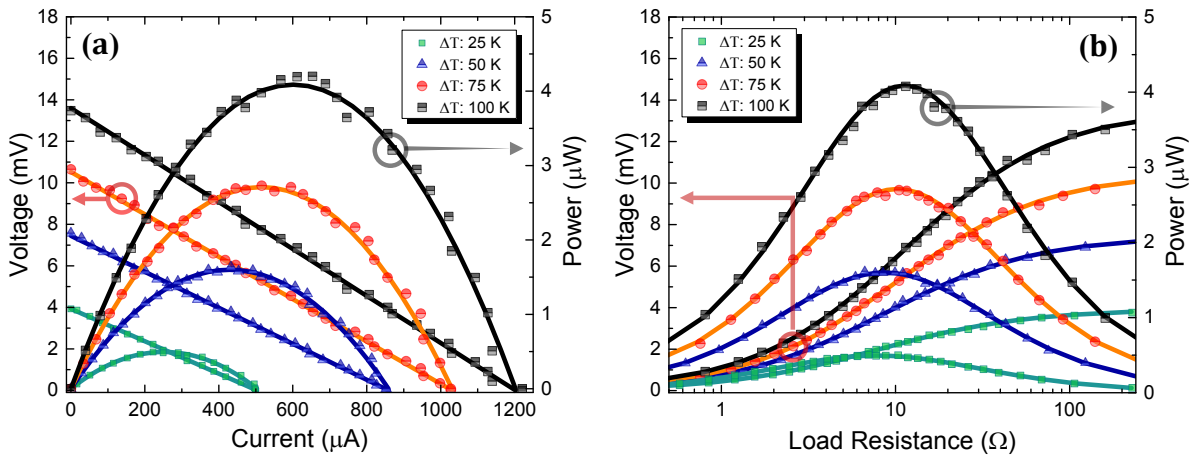


Figure 7. The experimentally measured thermoelectric performance of the 3D-CTEG in various ΔT s. (a) The obtained curves of Voltage-Current (V-I), Power-Current (P-I) and (b) Voltage-Load resistance (V- R_{LOAD}), Power-Load resistance (P- R_{LOAD}).

The power density of the 3D-CTEG module could be calculated using the equation [48].



$$P_{density} = \frac{P_{max}}{N \cdot A} = \frac{(N \cdot S \cdot \Delta T)^2 / 4 \cdot N \cdot \frac{l}{\sigma \cdot w \cdot d}}{N \cdot w \cdot d} = \frac{S^2 \cdot \sigma}{4l} \cdot \Delta T^2 \quad (3)$$

View Article Online
DOI: 10.1039/D4YA00182F

where N represents the number of the thermoelements, A is the area of the thermoelement, w is the width, d is the thickness and l is the length of the thermoelements. The power density of the 3D-CTEG was calculated at 256 mW/m^2 and the specific power at $205 \text{ } \mu\text{W/g}$, both of which are amid the highest values reported for flexible 3D-printed TEGs [7, 34, 43, 49, 50].

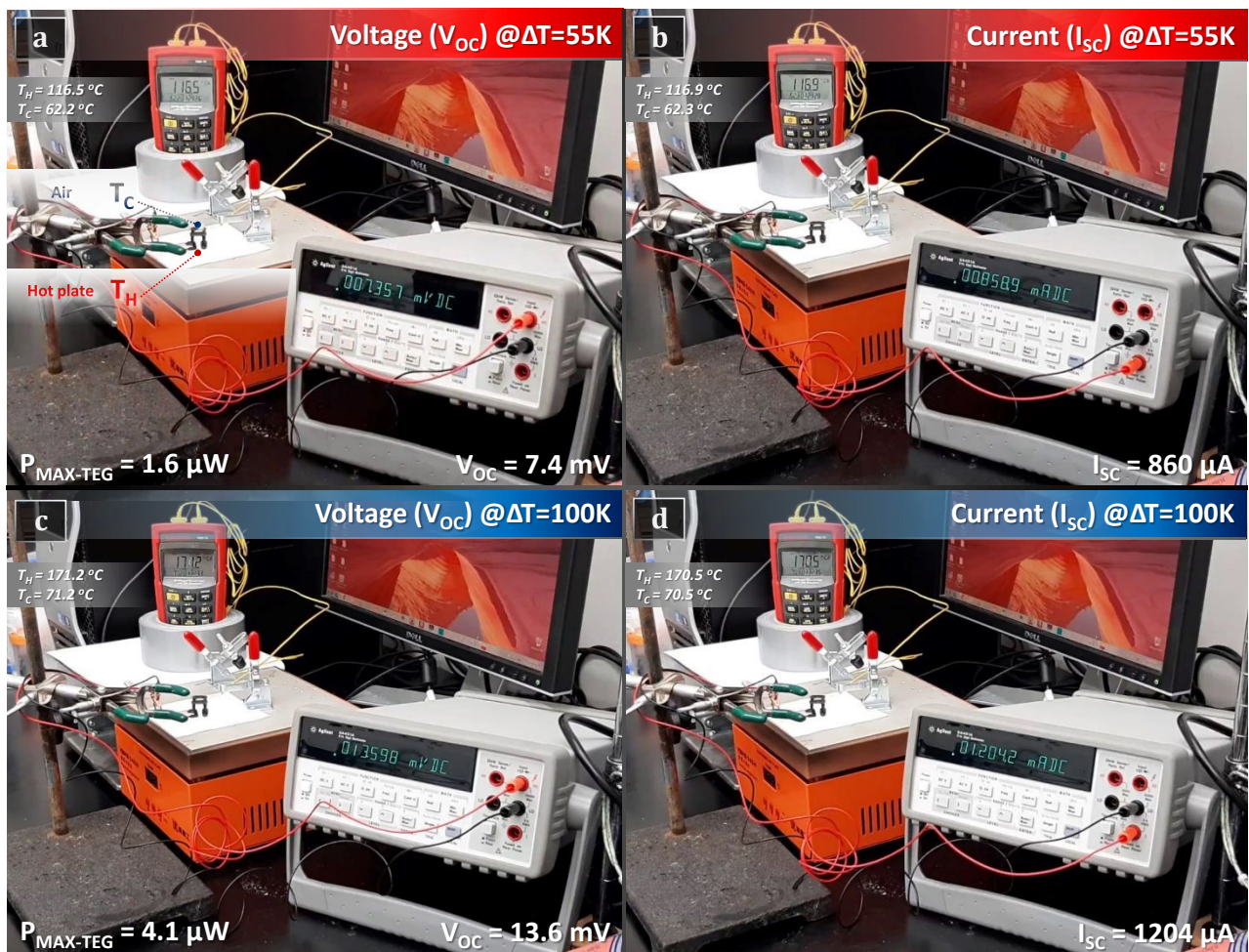


Figure 8. 3D-CTEG-device performance. The generated open-circuit voltage (V_{OC}) and short-circuit current (I_{SC}) at (a) $\Delta T=55\text{K}$ and (b) at $\Delta T=100\text{K}$.

3.6. Flexibility performance of the 3D-CTEG structure

Quantitative assessment of the bending radius of the manufactured structure was performed by bending the 3D-CTEG device. The flexibility of the TEG device is quite important for the endurance and integrity of the module's performance and functionality. Additionally, it could be useful to understand the possibilities and limitations for the device to be applicable to heat sources with irregular surfaces to take advantage of the ubiquitous heat dissipation. Conventional π -type TE modules consist of p-/n-type TE materials electrically interconnected in-series via metal contacts. Furthermore, numerous gold or silver nanometers are often placed as top electrodes on each



thermoelement to minimize contact resistance. In contrast to a standard TEG configuration, our 3D-CTEG lacks rigid metallic contacts between p-type and n-type thermocouples, resulting in exceptional flexibility, as illustrated in Figure 9. Figure 9a depicts the variation of resistance $\Delta R/R_0$ of the manufactured 3D-CTEG as a function of bending radius ranging from 5 cm to 1 cm in the vertical (A-A') and horizontal axis (B-B'). The resistance variation ratio is expressed as $\Delta R/R_0$, where R_0 is the 3D-CTEG device's initial resistance and ΔR is the resistance change between the real-time resistance measured under specific function and R_0 ($\Delta R=R-R_0$). When the 3D-CTEG was flexed along A-A' and B-B' axes up to a radius of 1 cm, the structure's $\Delta R/R_0$ was 2.9% and 3.8%, respectively; contrary, the overall internal resistance change was trivial. Figure 9b depicts the $\Delta R/R_0$ versus the obtained voltage after numerous bending iterations with a radius of 2 cm. Following 500 bending cycles, the unit's $\Delta R/R_0$ values were 7.6% along the A-A' axis and 10.3% at the B-B' axis. During this time, the device's output voltage at $\Delta T=100^\circ\text{C}$ ($T_H=170^\circ\text{C}$), was nearly constant. The $\Delta R/R_0$ versus the device's temperature rise is shown in Figure 9c, where an almost linear trend is observed, with an average rise of 2.4% every 10°C . The 3D-CTEG's durability is demonstrated in Figure 9d, where the device's generated voltage and internal resistance both remained remarkably constant after a 100 heating cycle evaluation. In summary, the manufactured 3D-CTEG device is shown to have exceptional durability, stability, and flexibility, making it a reliable thermoelectric generator.

View Article Online
DOI: 10.1039/D4YA00182F

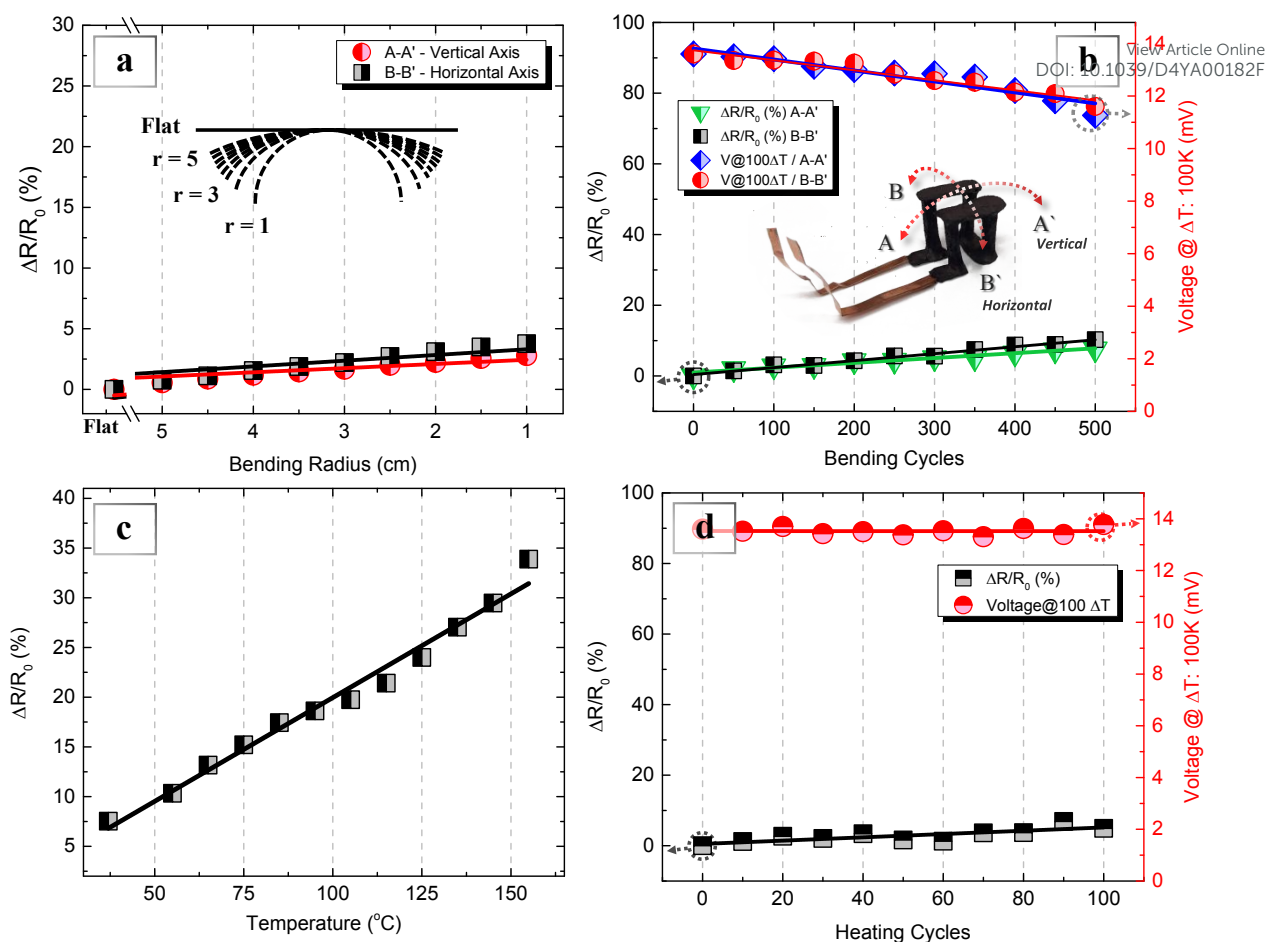


Figure 9. Flexibility measurements of the developed 3D-CTEG device. (a) Resistance variation ratios ($\Delta R/R_0$) of the CTEG while bending with different radii. (b) $\Delta R/R_0$ and voltage output in various bending cycles @ $\Delta T=100$ °C. (c) $\Delta R/R_0$ as a temperature function. (d) The repeatability of the $\Delta R/R_0$ as well as the voltage output of the CTEG over 100 heating cycles at $\Delta T =100^{\circ}C$. For (b-d) the bending radius was 2 cm.

4. Conclusions

This study has the aim to utilize additive manufacturing via DIW method to develop a carbon-based flexible 3D-printed thermoelectric generator and demonstrate its TE performance. The SWCNT/epoxy-based TE material employed for the printed TEG architecture is based on SWCNT/epoxy dispersions and produced via facile shear-mixing methods and low-cost materials. The manufactured 3D-CTEG consisted of two serially interconnected carbon-based p/n-pairs. Due to their excellent electrical conductivity, the SWCNT/epoxy-based printed TE structures were also adopted for connectors between the p/n- thermoelements. The dominant p- and n-type 3D-printed TE materials, demonstrated the substantial PFs of $102 \mu W/mK^2$ and $75 \mu W/mK^2$ respectively. The additively manufactured 3D-CTEG exhibited a $V_{OC}=13.6$ mV and an $I_{SC}=1204$ μA at $\Delta T=100K$ with an $R_{TEG}=11.3$ Ω . As an outcome, the noteworthy power output of $4.1 \mu W$ was achieved by only four thermoelements. The fabrication of a flexible 3D-CTEG with thermal energy harvesting capabilities is a key step toward sustainable and sophisticated zero-energy consumption components and



constructions. This particular thermoelectric device development approach could easily be adjusted in wearables (shoes, jacket insulation mesh), transportation (car hoods, heated parts of aircrafts or ships), and even existing power generation devices (basis of photovoltaic devices in direct contact with the panels, or even wind turbine thermal spots).

View Article Online
DOI: 10.1039/D4YA00182F

It is also a potentially efficient method for a broad range of applications, including distant places where powering low-energy consumption devices is required to give entirely energy independent solutions. The substantially obtained TE efficiency attained by the carbon-based 3D-TEG expands immense for large-scale 3D-printable and additive manufacturing processes of low-cost and efficient flexible thermoelectric generators, which might have a significant influence on the renewable energy sector.

Author contribution

C.K.M. was involved to the production processes of the thermoelectric materials, the device architecture, the principal idea and the implementation of the design, the manufacturing, and the characterization of the 3D-CTEG. W.J.W contributed to the 3D-printing additive manufacturing processes of the carbon-based TE materials. C.K.M., R.G., L.T. and G.K. involved to the thermoelectric and electrical characterization of the produced materials. C.K.M., A.S.P. and E.C. involved to the core idea development. C.K.M. and L.T. involved to the TGA measurements and analysis of the 3D-printed materials. C.K.M. involved to the SEM measurements, imaging and analysis. A.S.P. and E.C. also contributed to advising, reviewing, editing and supervise the entire study.

Acknowledgments

C.K.M. gratefully acknowledges the Fulbright Foundation and the Institute of International Education (iie) for financial support of this research at the College of Engineering of the University of Miami.

References

- [1] R. Sivaraj, P.K.S.M. Rahman, P. Rajiv, H.A. Salam, R. Venckatesh, Biogenic copper oxide nanoparticles synthesis using *Tabernaemontana divaricate* leaf extract and its antibacterial activity against urinary tract pathogen, *Spectrochimica Acta Part A: Molecular and Biomolecular Spectroscopy* 133 (2014) 178-181.
- [2] M.G. Kanatzidis, Chapter 3 The role of solid-state chemistry in the discovery of new thermoelectric materials, in: T.M. Tritt (Ed.), *Semiconductors and Semimetals*, Elsevier 2001, pp. 51-100.
- [3] A.J. Minnich, M.S. Dresselhaus, Z.F. Ren, G. Chen, Bulk nanostructured thermoelectric materials: current research and future prospects, *Energy & Environmental Science* 2(5) (2009) 466-479.
- [4] M. Aljaghtham, E. Celik, Design of cascade thermoelectric generation systems with improved thermal reliability, *Energy* 243 (2022) 123032.
- [5] G. Tan, L.-D. Zhao, M.G. Kanatzidis, Rationally Designing High-Performance Bulk Thermoelectric Materials, *Chemical Reviews* 116(19) (2016) 12123-12149.



- [6] X.-L. Shi, J. Zou, Z.-G. Chen, *Advanced Thermoelectric Design: From Materials and Structures to Devices*, *Chemical Reviews* 120(15) (2020) 7399-7515.
- [7] C. Oztan, S. Ballikaya, U. Ozgun, R. Karkkainen, E. Celik, Additive manufacturing of thermoelectric materials via fused filament fabrication, *Applied Materials Today* 15 (2019) 77-82. DOI: 10.1039/D4YA00182F
- [8] M. Aljaghtham, E. Celik, Energy conversion and thermal reliability of thermoelectric materials in unileg annular configuration, *Materials Letters* 300 (2021) 130192.
- [9] G. Zhou, D. Wang, Few-quintuple Bi₂Te₃ nanofilms as potential thermoelectric materials, *Scientific Reports* 5(1) (2015) 8099.
- [10] C.Y. Oztan, B. Hamawandi, Y. Zhou, S. Ballikaya, M.S. Toprak, R.M. Leblanc, V. Coverstone, E. Celik, Thermoelectric performance of Cu₂Se doped with rapidly synthesized gel-like carbon dots, *Journal of Alloys and Compounds* 864 (2021) 157916.
- [11] G.J. Snyder, A.H. Snyder, Figure of merit ZT of a thermoelectric device defined from materials properties, *Energy & Environmental Science* 10(11) (2017) 2280-2283.
- [12] Q. Jiang, J. Yang, P. Hing, H. Ye, Recent advances, design guidelines, and prospects of flexible organic/inorganic thermoelectric composites, *Materials Advances* 1(5) (2020) 1038-1054.
- [13] C.K. Mytafides, L. Tzounis, G. Karalis, P. Formanek, A.S. Paipetis, High-Power All-Carbon Fully Printed and Wearable SWCNT-Based Organic Thermoelectric Generator, *ACS Applied Materials & Interfaces* 13(9) (2021) 11151-11165.
- [14] G. Karalis, L. Tzounis, K. Tsirka, C.K. Mytafides, M. Liebscher, A.S. Paipetis, Carbon fiber/epoxy composite laminates as through-thickness thermoelectric generators, *Composites Science and Technology* (2022) 109291.
- [15] T. Juntunen, H. Jussila, M. Ruoho, S. Liu, G. Hu, T. Albrow-Owen, L.W.T. Ng, R.C.T. Howe, T. Hasan, Z. Sun, I. Tittonen, Inkjet Printed Large-Area Flexible Few-Layer Graphene Thermoelectrics, *Advanced Functional Materials* 28(22) (2018) 1800480.
- [16] F. Kim, B. Kwon, Y. Eom, J.E. Lee, S. Park, S. Jo, S.H. Park, B.-S. Kim, H.J. Im, M.H. Lee, T.S. Min, K.T. Kim, H.G. Chae, W.P. King, J.S. Son, 3D printing of shape-conformable thermoelectric materials using all-inorganic Bi₂Te₃-based inks, *Nature Energy* 3(4) (2018) 301-309.
- [17] R.R. Søndergaard, M. Hösel, N. Espinosa, M. Jørgensen, F.C. Krebs, Practical evaluation of organic polymer thermoelectrics by large-area R2R processing on flexible substrates, *Energy Science & Engineering* 1(2) (2013) 81-88.
- [18] Y. Jia, Q. Jiang, H. Sun, P. Liu, D. Hu, Y. Pei, W. Liu, X. Crispin, S. Fabiano, Y. Ma, Y. Cao, Wearable Thermoelectric Materials and Devices for Self-Powered Electronic Systems, *Advanced Materials* 33(42) (2021) 2102990.
- [19] J. Zang, J. Chen, Z. Chen, Y. Li, J. Zhang, T. Song, B. Sun, Printed flexible thermoelectric materials and devices, *Journal of Materials Chemistry A* 9(35) (2021) 19439-19464.
- [20] C. Navone, M. Soulier, M. Plissonnier, A.L. Seiler, Development of (Bi,Sb)₂(Te,Se)₃-Based Thermoelectric Modules by a Screen-Printing Process, *Journal of Electronic Materials* 39(9) (2010) 1755-1759.
- [21] A. Chen, D. Madan, P.K. Wright, J.W. Evans, Dispenser-printed planar thick-film thermoelectric energy generators, *Journal of Micromechanics and Microengineering* 21(10) (2011) 104006.
- [22] M. He, Y. Zhao, B. Wang, Q. Xi, J. Zhou, Z. Liang, 3D Printing Fabrication of Amorphous Thermoelectric Materials with Ultralow Thermal Conductivity, *Small* 11(44) (2015) 5889-5894.
- [23] D. Grossin, A. Montón, P. Navarrete-Segado, E. Özmen, G. Urruth, F. Maury, D. Maury, C. Frances, M. Tourbin, P. Lenormand, G. Bertrand, A review of additive manufacturing of ceramics by powder bed selective laser processing (sintering / melting): Calcium phosphate, silicon carbide, zirconia, alumina, and their composites, *Open Ceramics* 5 (2021) 100073.
- [24] M. Manoj Prabhakar, A.K. Saravanan, A. Haiter Lenin, I. Jerin leno, K. Mayandi, P. Sethu Ramalingam, A short review on 3D printing methods, process parameters and materials, *Materials Today: Proceedings* 45 (2021) 6108-6114.
- [25] Y. Yan, H. Ke, J. Yang, C. Uher, X. Tang, Fabrication and Thermoelectric Properties of n-Type CoSb_{2.85}Te_{0.15} Using Selective Laser Melting, *ACS Applied Materials & Interfaces* 10(16) (2018) 13669-13674.
- [26] Y. Mao, Y. Yan, K. Wu, H. Xie, Z. Xiu, J. Yang, Q. Zhang, C. Uher, X. Tang, Non-equilibrium synthesis and characterization of n-type Bi₂Te_{2.7}Se_{0.3} thermoelectric material prepared by rapid laser melting and solidification, *RSC Advances* 7(35) (2017) 21439-21445.
- [27] M. Smith, Z. Guan, W.J. Cantwell, Finite element modelling of the compressive response of lattice structures manufactured using the selective laser melting technique, *International Journal of Mechanical Sciences* 67 (2013) 28-41.
- [28] S. Iijima, Helical Microtubules of Graphitic Carbon, *Nature* 354 (1991) 56.



- [29] Y. Shi, C. Yan, Y. Zhou, J. Wu, Y. Wang, S. Yu, Y. Chen, Chapter 1 - Overview of additive manufacturing technology and materials, in: Y. Shi, C. Yan, Y. Zhou, J. Wu, Y. Wang, S. Yu, Y. Chen (Eds.), *Materials for Additive Manufacturing*, Academic Press 2021, pp. 1-8.
- [30] G. Karalis, L. Tzounis, E. Dimos, C.K. Mytafides, M. Liebscher, A. Karydis-Messimis, N.E. Zafeiropoulos, A.S. Paipetis, Printed Single-Wall Carbon Nanotube-Based Joule Heating Devices Integrated as Functional Laminae in Advanced Composites, *ACS Applied Materials & Interfaces* 13(33) (2021) 39880-39893.
- [31] C.K. Mytafides, L. Tzounis, G. Karalis, P. Formanek, A.S. Paipetis, Fully printed and flexible carbon nanotube-based thermoelectric generator capable for high-temperature applications, *Journal of Power Sources* 507 (2021) 230323.
- [32] G. Karalis, L. Tzounis, K. Tsirka, C.K. Mytafides, A. Voudouris Itskaras, M. Liebscher, E. Lambrou, L.N. Gergidis, N.-M. Barkoula, A.S. Paipetis, Advanced Glass Fiber Polymer Composite Laminate Operating as a Thermoelectric Generator: A Structural Device for Micropower Generation and Potential Large-Scale Thermal Energy Harvesting, *ACS Applied Materials & Interfaces* 13(20) (2021) 24138-24153.
- [33] Y. Nonoguchi, K. Ohashi, R. Kanazawa, K. Ashiba, K. Hata, T. Nakagawa, C. Adachi, T. Tanase, T. Kawai, Systematic Conversion of Single Walled Carbon Nanotubes into n-type Thermoelectric Materials by Molecular Dopants, *Scientific Reports* 3 (2013) 3344.
- [34] J.L. Blackburn, A.J. Ferguson, C. Cho, J.C. Grunlan, Carbon-Nanotube-Based Thermoelectric Materials and Devices, *Advanced Materials* 30(11) (2018) 1704386.
- [35] K. Chiou, S. Byun, J. Kim, J. Huang, Additive-free carbon nanotube dispersions, pastes, gels, and doughs in cresols, *Proceedings of the National Academy of Sciences* 115(22) (2018) 5703-5708.
- [36] K. Suganuma, *Introduction to Printed Electronics*, Springer, Osaka, Japan, 2014.
- [37] J. Choi, Y. Jung, S.J. Yang, J.Y. Oh, J. Oh, K. Jo, J.G. Son, S.E. Moon, C.R. Park, H. Kim, Flexible and Robust Thermoelectric Generators Based on All-Carbon Nanotube Yarn without Metal Electrodes, *ACS Nano* 11(8) (2017) 7608-7614.
- [38] G. Karalis, K. Tsirka, L. Tzounis, C. Mytafides, L. Koutsotolis, A.S. Paipetis, Epoxy/Glass Fiber Nanostructured p- and n-Type Thermoelectric Enabled Model Composite Interphases, *Applied Sciences* 10(15) (2020).
- [39] G. Karalis, C.K. Mytafides, L. Tzounis, A.S. Paipetis, N.-M. Barkoula, An Approach toward the Realization of a Through-Thickness Glass Fiber/Epoxy Thermoelectric Generator, *Materials* 14(9) (2021).
- [40] J.L. Blackburn, T.M. Barnes, M.C. Beard, Y.-H. Kim, R.C. Tenent, T.J. McDonald, B. To, T.J. Coutts, M.J. Heben, Transparent Conductive Single-Walled Carbon Nanotube Networks with Precisely Tunable Ratios of Semiconducting and Metallic Nanotubes, *ACS Nano* 2(6) (2008) 1266-1274.
- [41] R.C. Tenent, T.M. Barnes, J.D. Bergeson, A.J. Ferguson, B. To, L.M. Gedvilas, M.J. Heben, J.L. Blackburn, Ultrasoft, Large-Area, High-Uniformity, Conductive Transparent Single-Walled-Carbon-Nanotube Films for Photovoltaics Produced by Ultrasonic Spraying, *Advanced Materials* 21(31) (2009) 3210-3216.
- [42] S.G. King, L. McCafferty, V. Stolojan, S.R.P. Silva, Highly aligned arrays of super resilient carbon nanotubes by steam purification, *Carbon* 84 (2015) 130-137.
- [43] W. Zhou, Q. Fan, Q. Zhang, L. Cai, K. Li, X. Gu, F. Yang, N. Zhang, Y. Wang, H. Liu, W. Zhou, S. Xie, High-performance and compact-designed flexible thermoelectric modules enabled by a reticulate carbon nanotube architecture, *Nature Communications* 8(1) (2017) 14886.
- [44] J.-H. Mo, J.-Y. Kim, Y.H. Kang, S.Y. Cho, K.-S. Jang, Carbon Nanotube/Cellulose Acetate Thermoelectric Papers, *ACS Sustainable Chemistry & Engineering* 6(12) (2018) 15970-15975.
- [45] G.J. Snyder, E.S. Toberer, Complex thermoelectric materials, *Nature Materials* 7(2) (2008) 105-114.
- [46] R.S. Prasher, X.J. Hu, Y. Chalopin, N. Mingo, K. Lofgreen, S. Volz, F. Cleri, P. Keblinski, Turning Carbon Nanotubes from Exceptional Heat Conductors into Insulators, *Physical Review Letters* 102(10) (2009) 105901.
- [47] Y. Lan, Y. Wang, Z. Ren, Physics and applications of aligned carbon nanotubes, *Advances in Physics - ADVAN PHYS* 60 (2011) 553-678.
- [48] Y. Lu, Y. Ding, Y. Qiu, K. Cai, Q. Yao, H. Song, L. Tong, J. He, L. Chen, Good Performance and Flexible PEDOT:PSS/Cu₂Se Nanowire Thermoelectric Composite Films, *ACS Applied Materials & Interfaces* 11(13) (2019) 12819-12829.
- [49] M.-H. Lee, Y.H. Kang, J. Kim, Y.K. Lee, S.Y. Cho, Freely Shapable and 3D Porous Carbon Nanotube Foam Using Rapid Solvent Evaporation Method for Flexible Thermoelectric Power Generators, *Advanced Energy Materials* 9(29) (2019) 1900914.
- [50] D. Zhang, W.Y.S. Lim, S.S.F. Duran, X.J. Loh, A. Suwardi, Additive Manufacturing of Thermoelectrics: Emerging Trends and Outlook, *ACS Energy Letters* 7(2) (2022) 720-735.

View Article Online

DOI: 10.1039/D4VA00182F

